Published in final edited form as:
Methods Cell Biol. 2012 ; 108: 367–393. doi:10.1016/B978-0-12-386487-1.00017-1.

Analysis of cholesterol trafficking with fluorescent probes

Frederick R. Maxfield[1] and **Daniel Wüstner**[2]

[1]Department of Biochemistry, Weill Cornell Medical College, 1300 York Ave., New York, NY 10065, USA

[2]Department of Biochemistry and Molecular Biology, University of Southern Denmark, DK-5230 Odense M, Denmark

Abstract

Cholesterol plays an important role in determining the biophysical properties of biological membranes, and its concentration is tightly controlled by homeostatic processes. The intracellular transport of cholesterol among organelles is a key part of the homeostatic mechanism, but sterol transport processes are not well understood. Fluorescence microscopy is a valuable tool for studying intracellular transport processes, but this method can be challenging for lipid molecules because addition of a fluorophore may alter the properties of the molecule greatly. We discuss the use of fluorescent molecules that can bind to cholesterol to reveal its distribution in cells. We also discuss the use of intrinsically fluorescent sterols that closely mimic cholesterol, as well as some minimally modified fluorophore-labeled sterols. Methods for imaging these sterols by conventional fluorescence microscopy and by multiphoton microscopy are described. Some label-free methods for imaging cholesterol itself are also discussed briefly.

Keywords

Fluorescence microscopy; multiphoton microscopy; filipin; cholesterol; dehydroergosterol; cholestatrienol; BODIPY-cholesterol

Introduction

Cholesterol is an essential component of mammalian cell membranes, and it plays an important role in determining the biophysical characteristics of these membranes [1, 2]. The concentration of cholesterol varies greatly among organelles with levels around 30% of the lipid molecules in the plasma membrane and about 5% in the endoplasmic reticulum. Cholesterol is transported among organelles by a mixture of vesicular and non-vesicular transport processes, and the mechanisms regulating this transport are only partially understood. Cholesterol transport in cells can be studied by following radiolabeled cholesterol, but this requires stringent purification of organelles under conditions in which the sterol does not redistribute. Contamination with a small fraction of membranes with high cholesterol content can lead to significant errors in measurements of cholesterol content in organelles such as the endoplasmic reticulum.

Fluorescence microscopy has been a powerful tool for studying the intracellular transport of proteins. A difficulty in studying transport of cholesterol (and other lipids) using microscopy

Correspondence: Frederick R. Maxfield, Department of Biochemistry, Room E-215, Weill Cornell Medical College 1300 York Ave., New York, NY 10065, USA, Tel: (1) 212 746 6405, Fax: (1) 212 746 8875, frmaxfie@med.cornell.edu Or Daniel Wüstner, Department of Biochemistry and Molecular Biology, University of Southern Denmark, DK-5230, Odense M, Denmark, Tel.: (45) 6550 2405, Fax: (45) 6550 2467, wuestner@bmb.sdu.dk.

is that coupling to a fluorophore can dramatically change the properties of the molecule and its interactions with other components of the membrane. Recently, two types of approaches for studying fluorescent sterols have been implemented. One approach has been to use an added fluorophore selected to minimize the perturbation as compared to cholesterol itself. Bora-diaza-indacene (BODIPY) -cholesterol (Figure 1) has been used as a cholesterol probe in model membranes and in trafficking studies in living cells [3–7]. The second approach takes advantage of intrinsically fluorescent sterols (Figure 1) [8–13], including dehydroergosterol (DHE; a natural sterol found in yeast) and cholestatrienol (CTL; a synthetic sterol that is close to cholesterol in its structure and in many of its biophysical properties). Both of these fluorescent sterols have two additional double bonds in the steroid rings, which creates the fluorophore. Fluorescent sterols can be added to cells either by delivery to the plasma membrane or incorporated into reconstituted lipoproteins. The movement of the sterols through the cells can then be observed directly, or they can be used for techniques such as fluorescence recovery after photobleaching to determine transport kinetics [8, 14,15].

In this chapter, we discuss the relative merits of these fluorescent sterols, and we discuss the methodology for their use. We also discuss some recent developments in the label-free detection of sterols in cells. We begin by discussing the use of fluorescent sterol-binding molecules that are useful for analyzing the distribution of cholesterol in fixed cells or tissues.

Visualization of cholesterol using sterol-binding probes

Sterol-binding natural products have been used to localize cholesterol in cells, and their use has been described in detail [16]. Filipin is a naturally fluorescent polyene antibiotic that binds to cholesterol but not to esterified sterols. Thus, it is useful for detecting free (i.e., unesterified) cholesterol in biological membranes. Filipin fluorescence is observed with UV excitation around 360 nm and emission around 480 nm. Filipin binding perturbs the bilayer structure, so filipin cannot be used on living cells. Beyond the free 3′-OH group, the exact basis for filipin's specificity is not fully understood. There are some important practical considerations in the use of filipin. Stock solutions in DMSO must be rigorously dried with Molecular Sieves to remove residual water. Filipin is rapidly photobleached with the UV light intensity available in most fluorescence microscopes. However, with a good camera, we have been able to attenuate the incident light using neutral density filters to 1–10% of the full brightness and obtain good images that photobleach slowly. Excessive photobleaching without the use of a neutral density filter is one of the greatest problems in reproducibility of results using filipin. Since the basis for filipin binding is not fully understood, it must be considered that there can be interfering effects. Nevertheless, we have been able to correlate brightness of filipin labeling with chemically measured cholesterol levels in cells in which cholesterol content was altered by incubation with methyl-β-cyclodextrin (MβCD) or with cholesterol:MβCD complexes [17]. Filipin treatment causes dimpling of the membrane that can be observed by electron microscopy [18]. It should be noted, however, that filipin deformation of the membrane can be affected by membrane:protein interactions [19]. A recent paper discussed the use of filipin to label brain sections from mice with lysosomal storage disorders [20]. It was found that in addition to cholesterol, filipin was also labeling the GM1 ganglioside. This points to the importance of verifying the validity of sterol-labeling reagents in each experimental system. In addition, particular care should be taken in cells that express large amounts of GM1.

Pore-forming cytolysins that bind to sterols have also been used to visualize cholesterol in cells. These polypeptide bacterial toxins bind to cholesterol in membranes and self-associate to form pores in the bilayer. For fluorescence microscopy the toxins can be labeled with a fluorescent dye and imaged with filter sets appropriate for the dye. Some investigators have

preferred the use of these toxins, including perfringolysin-O or a biotinylated derivative of this called BCθ-toxin, because the fluorescent dyes (or the labeled avidin for BCθ-toxin) are more photostable than filipin. One issue is that the perfringolysin-O binding to membranes increases very non-linearly as cholesterol content increases [21]. It appears that the binding is preferentially to cholesterol molecules with a high chemical activity coefficient. The cholesterol content at which the rapid increase in binding is observed depends on the lipid content of the membrane. For ER lipids, this occurs at about 5% cholesterol, but in other membranes binding is seen above 20% cholesterol [16].

Automated microscopy for cholesterol high throughput screens

Filipin labeling has been used for many years for diagnosis of Niemann-Pick Disease type C (NPC), an inherited disorder leading to cholesterol accumulation in lysosomal storage organelles (LSOs), which are modified late endosomes and lysosomes [22]. Recently, filipin labeling of the cholesterol accumulation in LSOs has been used for high throughput automated microscopy screening of compounds that might reduce the cholesterol accumulation [23, 24]. In this application imaging is essential because the total cholesterol level in the NPC mutant cells does not change greatly. Nevertheless, differences caused by the mutation are easily quantified by microscopy because the filipin-labeled LSOs accumulate in the peri-nuclear region, while the rest of the cell actually has lower cholesterol levels than normal cells [23].

Cells are plated in 384-well plates, treated with various concentrations of test compounds, fixed with 1.5% paraformaldehyde, and labeled with 50 μg/ml filipin (from a 25 mg/ml stock in dry DMSO) in phosphate buffered saline (PBS) for 45 minutes. The cells are then rinsed and imaged on an automated microscopy system (ImageXpress^{Micro} from Molecular Devices or equivalent) using UV excitation and a dry 10x objective. Automated image analysis is used to quantify the fluorescence power per cell in areas that are above a threshold brightness corresponding to the brightness in LSOs of untreated cells. Further details are provided elsewhere [23, 24]. Screens based on this procedure have identified compounds that reduce the cholesterol levels in NPC mutant cells by various mechanisms [24–27].

Biophysical properties of cholesterol and its fluorescent analogs

Valid fluorescent analogs of cholesterol should reproduce its biophysical interactions with lipids in the bilayer as closely as possible. Cholesterol has a small headgroup (the 3′-β-hydroxyl group) that can create hydrogen bonds to other lipid headgroups in the interfacial region of the bilayer, while its hydrophobic steroid ring system and isooctyl side chain are buried in the hydrophobic region of the membrane [28–30]. Cholesterol molecules are shielded under the phospho- and sphingolipid headgroups, thereby minimizing contact with water molecules. This shielding, together with attractive van der Waals interactions with neighboring acyl chains, causes lipid membranes to have a reduced area in the presence of cholesterol. This property is described as cholesterol's condensing effect [30–32].

When cholesterol is added to a membrane consisting of phospholipids with saturated acyl chains, (e.g., dipalmitoylphosphatidylcholine) below the phase transition temperature of the phospholipid, the sterol will perturb the high structural order in the liquid-crystalline state [33]. In contrast, when added to membranes in the liquid-disordered (I_d) phase, cholesterol has an ordering effect, and it can induce a liquid-ordered (I_o) phase at high sterol mole fractions (approx. above 30 mol% - i.e., 30% of the lipid molecules) [34]. The I_o phase is characterized by high lateral lipid mobility, straightened acyl chains and tight lipid packing. The I_o phase has attracted interest, due to similar properties observed in cellular membranes [35–37]. Despite this resemblance, it has to be emphasized that the I_o phase is strictly

defined only for simple two and three-component lipid mixtures at thermodynamic equilibrium. Partitioning of fluorescent sterols between I_o and I_d phase as well as their potential to induce the I_o phase can be used as criteria to assess their potential as cholesterol mimic [7, 38, 39].

Properties of fluorescent sterols

a) Dehydroergosterol and Cholestatrienol—Both intrinsically fluorescent sterols, DHE and CTL, contain three conjugated double bonds in the steroid ring system giving these probes their slight fluorescence in the near UV-region of the spectrum. Since they contain an identical chromophore, the photo-physical properties of DHE and CTL are nearly identical [40–43]. Both sterols have excitation and emission maxima in membranes of λ_{ex} = 320 nm and λ_{em} = 370–400 nm [10, 41, 44, 45]. The fluorescence lifetime of both sterols is short, around τ_f = 0.3 – 0.8 ns in various organic solvents and lipid membranes at room temperature [40, 42, 45, 46]. Low extinction coefficient ($\varepsilon \approx 11{,}000\ M^{-1} \cdot cm^{-1}$) and quantum yield ($\Phi_f$ = 0.04 in ethanol) results in low fluorescence brightness of these sterols. The environmental sensitivity of DHE and CTL is low since the molecular dipole does not change greatly during electronic transition from the ground S_0, state to the excited S_1 state [42, 43, 45, 46]. In dimyristoylphosphatidylcholine liposomes, the fluorescence lifetime, τ_f, of DHE decreases in a sigmoidal fashion from τ_f = 2 ns at 10° C to τ_f = 0.5 ns at 42° C [42]. It has been reported that DHE and CTL self-quench at increasing mole fractions in phosphatidylcholine model membranes, as indicated by a drop in fluorescence intensity [44, 47]. Since no change in fluorescence lifetime was observed in these studies, it is likely that the proposed self-quenching is caused by static quenching [48]. By measuring fluorescence intensity of DHE in giant unilamellar vesicles (GUVs), we found no evidence for self-quenching but instead a linear relationship between DHE's emission and the mole fraction in the membranes [38]. Thus, quenching effects, which could complicate analysis of sterol distribution by fluorescence microscopy of DHE or CTL are unlikely, but systematic studies with varying lipid composition might be necessary to rule out any sterol self-quenching at concentrations used for studies in cells. Fluorescence anisotropy and quantum yield of DHE are very temperature-sensitive and much lower in membranes above than below the phase transition temperature [40, 42, 46]. Accordingly, under live cell imaging conditions the fluorescence brightness of both sterols should be further reduced. Another unfortunate property of DHE and CTL, at least for cellular imaging, is the high photobleaching propensity of these probes. How this can be avoided or used to advantage for microscopic investigation will be discussed later in this chapter.

Due to their minimal chemical alterations, DHE and CTL resemble the natural sterols ergosterol and cholesterol very closely. DHE differs from ergosterol only in one double bond, while CTL contains two more double bonds in the ring system than cholesterol. Accordingly, DHE is a naturally occurring sterol in yeast and red sponges, and it is the ideal mimic of ergosterol. CTL is the closest analog of cholesterol [41, 49]. The close resemblance of DHE and CTL to ergosterol and cholesterol is reflected by their biophysical properties in model membranes. DHE can, like ergosterol and cholesterol, induce the I_o phase in ternary lipid mixtures and partitions with high preference into that phase [38]. CTL also prefers the I_o over the I_d phase in GUV membranes [50]. CTL has a very similar potential to order acyl chains in membranes as cholesterol even at high sterol mole fraction, while DHE is slightly less efficient [51]. Similarly, DHE (like ergosterol, but in contrast to cholesterol) shows a concentration saturation effect in various biophysical effects on lipid membranes. That means that bilayer properties such as bending elasticity and ordering of phospholipid acyl chains depend on sterol mole fraction only up to about 10 mol% DHE in the membranes [32, 38, 51, 52]. In contrast, acyl chain ordering was found to depend linearly on cholesterol and CTL concentrations in the membrane, even at high sterol mole

fractions [32, 51]. The less flexible side chain of DHE and ergosterol as compared to CTL and cholesterol is likely responsible for this difference. We found that DHE and CTL have very similar intracellular trafficking itineraries to cholesterol, suggesting that the minor differences in biophysical properties of the analogs are not determining their overall transport in mammalian cells [53–55]. Interestingly, in a study in yeast cells, we observed different metabolism of DHE and ergosterol compared to cholesterol, indicating that DHE is the most suitable sterol analog in organisms containing ergosterol [56].

b) BODIPY-cholesterol—Recently, cholesterol analogs containing a BODIPY fluorophore have been synthesized by Bittman and co-workers [57]. The BODIPY moiety is particularly suitable for fluorescent lipid probes since it is relatively non-polar, allowing for insertion of the analogs into the hydrophobic interior of lipid membranes [58]. The BODIPY dye is electrically neutral, has a low environmental sensitivity, low Stokes shift (typically, λ_{ex} = 505 nm and λ_{em} = 515 nm), high extinction coefficient and high quantum yield ($\Phi_f \approx$ 0.9 in organic solvents) [59]. Several BODIPY dyes exhibit a red-shifted excited-state dimer (excimer) at high concentration in membranes [60–62]. This has been used to determine lateral clustering and sorting of these lipid probes in cells by quantitative fluorescence microscopy [61, 63–65]. BODIPY-cholesterol (BChol) with the dye at carbon 24 of the sterol side chain is a promising new cholesterol analog, which can supplement the well-established intrinsically fluorescent probes DHE and CTL [3–7]. BChol partitions preferentially into the I_o phase compared to the I_d phase in various ternary lipid mixtures [4, 6], though a direct comparison with DHE revealed that the latter sterol has an even higher preference for the I_o phase [7]. Since Bchol is more than 500-fold brighter than DHE, it can be used at very low concentrations (about 0.1–0.5 mol% of lipids) [3, 7]. In contrast, visualization of DHE in cells may require replacing up to 5% of the sterols [7, 15]. BChol has been used to investigate cholesterol mobility in the I_o and I_d phase in GUV's made of dioleoylphosphatidylcholine, egg yolk sphingomyelin and cholesterol [6]. The BODIPY-moiety of this BChol is oriented perpendicular to the bilayer normal (and the acyl chains), as measured by two-photon fluorescence polarization [6, 39], and the strength of this orientation is enhanced in the presence of cholesterol in the membranes [39]. BChol self-quenches at concentrations above 3 mol% in lipid membranes, but it does not form red-shifted excimers [7]. Instead, dark ground state dimers seem to be responsible for the self-quenching effect, as reported for some other BODIPY-tagged probes [7, 59, 66]. Molecular dynamics simulations of BChol indicate that it has a higher molecular tilt compared to cholesterol [3]. This can affect the local lipid structure surrounding the probe and might contribute to its lower partition into the I_o phase compared to DHE [3, 7]. The molecular tilt has been proposed to be a main determinant of the ability of a sterol to order phospholipid acyl chains and condense lipid bilayers [67]. For the intrinsically fluorescent sterols, DHE and CTL, the order parameter, S, which is inversely related to the molecular tilt, could be measured by fluorescence polarization spectroscopy, since the transition dipole of these sterols lies along the long molecular axis [42, 46]. The order parameter was found to be only a little lower for DHE compared to cholesterol (S = 0.67 for DHE and S = 0.85 for cholesterol in dimyristoylphosphatidylcholine at 37°C)[46, 68, 69].

c) NBD- and Dansyl-cholesterol—Cholesterol tagged with a 7-Nitrobenz-2-Oxa-1,3-Diazole (NBD)-group at carbon 22 or carbon 25 has been used in model membrane and cellular trafficking studies in yeast and in mammalian cells [4,13, 51, 70, 71]. A problem with these probes is their up-side down orientation in model membranes compared to cholesterol and intrinsically fluorescent sterols, as well as their low ordering capacity and partitioning into the I_d phase in ternary model membranes [51, 72]. NBD-cholesterol with the fluorophore at carbon 25 has been shown to be mistargeted in cells to mitochondria [13]. Dansyl-cholesterol is another fluorescent cholesterol analog used in cellular studies [73, 74].

The Dansyl moiety was linked to carbon 6 of the steroid ring system, and recent fluorescence studies found that the Dansyl-group of this sterol is localized on average 1.56 nm from the bilayer center [75]. This should significantly affect the lipid acyl chain packing in proximity of this probe when inserted into membranes. Partitioning of Dansyl-cholesterol between I_o and I_d phases in model membranes has not been reported. Quantitative studies of intracellular sterol distribution based on fluorescence of NBD- and Dansyl-cholesterol are also hampered by the high environmental sensitivity of the attached fluorophores. Accurate measurement of sterol distribution requires that emitted fluorescence is proportional to probe concentration, and this is not likely for these cholesterol probes [76]. Further details about NBD- and Dansyl-cholesterol can be found elsewhere [16, 49].

Transport of fluorescent cholesterol probes in cells

Live-cell imaging of intrinsically fluorescent sterols—Both DHE and CTL are suitable for studies in living cells. DHE is widely available from commercial sources, although concerns have been expressed about the purity of this material, which may vary depending on the supplier and the lot number [12]. CTL is not available commercially, but the method for synthesis has been published [77, 78]. Like many lipids, these fluorescent sterols are subject to oxidation, so they should be protected from exposure to air (e.g., by purging solvents with argon). They are also sensitive to light and should be stored in the dark. The purity can be checked by HPLC [12]. Of particular concern, oxidized DHE or CTL may affect the structure of lipid bilayers.

Several methods have been used to incorporate DHE or CTL into cells. For simplicity, we will describe methods for DHE, but the same methods would apply for CTL. The simplest method is to inject DHE in an ethanolic stock solution into the culture medium. The DHE is very poorly soluble in water; some of it will adsorb to serum proteins, but most will form microcrystals. These microcrystals may be taken up by the cells and slowly dissolved to allow the DHE to distribute into cell membranes. In our experience, this procedure results in very heterogeneous labeling of cells and incomplete breakup of the microcrystals. A much better procedure involves preparation of DHE complexes with MβCD, which solubilizes the sterol and allows it to be rapidly exchanged into the plasma membrane (Box 2). Sterol: MβCD complexes form at a 1:2 ratio [79], but these complexes can dissociate rapidly. Thus, it is necessary to maintain an excess of the MβCD in order to store sterol: MβCD complexes without precipitation of the DHE.

Box 2

Formation of DHE: MβCD complexes and labeling of cells

Dissolve 5 mg of DHE in 2.5 ml of ethanol to give a 5 mM stock solution. Transfer to a 30 ml clean glass vial and evaporate the ethanol under argon to produce a thin film. Add 2.5 ml of 25 mM MβCD in buffered saline to get a DHE/MβCD ratio of 1:5. Vortex repeatedly to resuspend the DHE film. (Warming to 37° C may help to release the dried film.) Sonicate for 10 min, and then shake at 37°C overnight. Centrifuge for 10 min at 21,000 × g to remove undissolved DHE, and then aliquot and store at 4°C under argon. The solution can be used for labeling the cells without further dilution. The labeling solution can be stored at 4°C, but it should be centrifuged to remove DHE crystals just before use.

Cells are rinsed and incubated with the labeling solution at 37°C for 0.5–1 minute to allow exchange of the DHE into the plasma membrane. The cells are then rinsed and returned to culture medium.

In normal cell physiology, cholesterol is delivered to cells as cholesteryl esters in the core of lipoproteins. DHE-oleate esters can be synthesized and incorporated into the core of reconstituted LDL [14]. Established procedures for reconstituting LDLcan be modified to incorporate DHE-oleate into the core of LDL or acetylated-LDL [80]. We have used this method to incorporate a mixture of DHE-oleate and cholesteryl-oleate into acetylated-LDL at a molar ratio of 1:10, using 6 mg of total neutral lipid per 1.9 mg of AcLDL protein [14].

The LDL can be taken into cells by receptor-mediated endocytosis via the LDL receptor. For uptake by macrophages, the reconstituted LDL can be acetylated, and the acetylated-LDL is taken up via scavenger receptor type A. The esters are hydrolyzed in late endosomes and lysosomes, releasing the unesterified DHE. We have verified that DHE esters are hydrolyzed, transported out of the digestive organelles, and distributed among cellular membranes [14]. DHE and CTL are also effective substrates for the esterifying enzyme, ACAT, which forms steryl esters that are incorporated into cytoplasmic lipid droplets, and these can be visualized in cells [14].

Although in this chapter we emphasize studies of mammalian cells in culture, *Caenorhabditis elegans* can be labeled with DHE by dietary feeding [81, 82]. The yeast, *Saccharomyces cerevisiae,* can also take up DHE when grown under hypoxic conditions [83], and the distribution and transport of the DHE can be analyzed by microscopy. For yeast, DHE is a naturally formed sterol, and it is also a natural component of the diet of *Caenorhabditis elegans.*

Measurement of transport kinetics by fluorescence recovery after photobleaching—Photobleaching of DHE can be a problem when several frames of the same field of view are acquired (e.g., in time-lapse imaging or when determining the effect of a drug or fluorescence quencher). Photobleaching of DHE can be used to advantage, however, for dynamic measurements of sterol transport. After selectively destroying DHE fluorescence by illumination of only a small region with closed field aperture on a wide field microscope, fluorescence recovery of DHE into that region was measured over time with the field aperture opened to image the whole cell [8, 14, 15, 84]. To quantify fluorescence recovery, DHE intensity in the bleached region was normalized to total cell intensity, thereby correcting for fluorescence loss during repeated acquisition.

Transbilayer distribution of fluorescent sterols—Transbilayer asymmetry is a general feature of most lipids in the plasma membrane and many other organelles. This asymmetry has important consequences for membrane physical properties and cell signaling. Although cholesterol is a major lipid in these membranes, its transbilayer distribution is not well understood. Fluorescent sterols such as DHE and CTL can be used with fluorescence quenchers that do not cross the bilayer to determine the sterol asymmetry in membranes [12, 55, 85]. In most such studies, it has been found that the abundance of DHE is greater on the cytoplasmic leaflet of the plasma membrane than on the exofacial leaflet. Using imaging methods described here, it is also possible to examine the DHE transbilayer distribution in organelles. When the membrane impermeant quencher, trinitrobenzene sulfonic acid, was microinjected into DHE-labeled cells, about 60% of the fluorescence in both the endocytic recycling compartment and the plasma membrane was quenched [54]. When the trinitrobenzene sulfonic acid was added outside the cell, only 20–30% of the fluorescence was quenched.

Metabolism of DHE in cells—DHE-oleate that is delivered to lysosomes in the core of LDL particles is hydrolyzed, presumably by lysosomal acid lipase, the lysosomal enzyme that hydrolyzes cholesteryl esters [14]. DHE is also esterified by the endoplasmic reticulum enzyme, ACAT, and stored in lipid droplets. Esterification of DHE can be verified by

extracting cellular neutral lipids and using HPLC to quantify free and esterified DHE [3, 14]. Incorporation into lipid droplets can be measured by fluorescence microscopy by determining the co-localization of DHE with a lipid droplet vital stain such as Nile Red or Lipidtox [7, 14, 86]. While DHE mimics many aspects of cholesterol in cells, it is not recognized by the regulatory proteins, SCAP and Insig, in the endoplasmic reticulum (A. Radhakrishnan, pers. comm.).

Imaging modalities for visualization of intrinsically fluorescent sterols

UV-sensitive wide field imaging—Excitation of DHE requires UV wavelengths around 330 nm, and the emission is around 400 nm. Both of these wavelengths impose special requirements as compared to typical epi-fluorescence microscopy. Most fluorescence microscopes contain glass elements that block transmission of light below 340 nm, and this greatly diminishes the excitation of DHE unless modifications are made. The most important modification is in the lamp housing. Conventional collecting lenses are a few cm thick, and they completely block transmission at 330 nm. Most research grade microscopes can be modified to incorporate UV-transmitting collecting lenses. An issue with single element collecting lenses is that the focal points for UV and visible wavelengths are very different, so optimal Köhler illumination cannot be obtained for the visible and UV simultaneously. We have obtained a multi-lens collector from Leica that corrects illumination adequately for wavelengths from 335 nm to 630 nm. If fiber optical systems are used for excitation, it is essential to verify that they have high transmittance at 330 nm.

Dichroic filter cubes for DHE imaging are available from various suppliers. We have used 335 nm (20 nm bandpass) excitation filter/365 nm longpass dichromatic filter/405 nm (40 nm bandpass) emission filter from Chroma (Brattleboro, VT). A microscope objective must also be chosen that has significant transmission below 340 nm. Finally, various glass elements in the optical path must be checked for transmission at 330 nm and replaced if necessary. For example, some infrared-blocking (heat) filters have poor transmission at 330 nm and must be replaced.

Because DHE fluorescence is weak and in the near UV, it places special requirements on the detector. The sensitivity of many CCD cameras falls off sharply around 400 nm, but detectors are available with coatings that extend sensitivity into the near UV. An important development is the availability of near-UV sensitive electron multiplying CCD (EMCCD) cameras. These cameras can provide a large increase in signal-to-noise ratio for detecting DHE as compared to previous versions of commercially available cameras. Using these near-UV sensitive EMCCD cameras, excitation light intensity can be reduced by 80–90% while still obtaining high quality images with less than 1 sec exposure time. This allows repeated observations of the same cell for time course studies or for obtaining images at multiple focal positions.

Image post processing for UV-sensitive wide field microscopy of DHE and CTL—Despite the advances in imaging technology described above, reliable detection of subcellular DHE and CTL distribution remains a challenge due to the weak fluorescence of these sterol probes. One potential problem of wide field imaging is a significant contribution of out-of-focus light [87]. Image restoration methods based on deconvolution can improve both axial and lateral resolution in wide field fluorescence images [87–89]. The performance of any deconvolution algorithm is limited by spherical aberration, image noise and by photobleaching of the fluorophore as multiple images are obtained at different focal planes [89, 90]. We have shown that iterative deconvolution in combination with photobleaching correction can significantly improve the performance of DHE imaging (see Fig. 2) [86].

Chromatic aberration caused by the wavelength dependence of the microscope optical glass elements is a potential problem in multicolor imaging with DHE and organelle markers. While good research objectives are normally corrected for chromatic aberration in the visible range of the spectrum, they fail to collect UV light at the same focal position as red and green light. This can be corrected for by acquiring z-stacks of multicolor fluorescent beads, measuring the axial and lateral off-set between the UV channel and red or green channels and correcting for these off-sets in a post-processing step [86]. Software has been developed that performs a non-linear regression of various decay models to photobleaching-induced intensity loss on a pixel-by-pixel basis [82]. This analysis revealed that DHE bleaches homogenously throughout cells, in stark contrast to other fluorescently labeled sterols, for example NBD-cholesterol [76, 82]. Moreover, DHE bleaching follows a simple mono-exponential decay, and the measured decay rate is comparable in model and cellular membranes and quite independent of DHE intensity [82]. Accordingly, bleach-rate imaging can be used as a fingerprint to detect DHE in the presence of other spectrally indistinguishable fluorophores. For example, we showed that bleach-rate imaging of DHE allows for selective detection of sterol enriched tissue in *Caenorhabditis elegans* despite the presence of significant autofluorescence [82, 91].

Multiphoton microscopy—As an alternative to conventional epifluorescence microscopy, intrinsically fluorescent sterols can be monitored in cells using multiphoton (MP) excitation. In this imaging modality, almost simultaneous absorption of two or more photons causes an electronic transition in the fluorophore from the ground to the first excited state. The absorbed photons have approximately one-half (for two-photon excitation) or one-third of the energy (for three-photon excitation) compared to the one-photon excitation process. Thus, as a rough rule of thumb, excitation of a fluorescent probe by two- or three-photon microscopy can be stimulated using twice or three times the wavelength used for one-photon excitation. For example, DHE is excited around 320 nm by a one-photon process, and it can be excited with 920 nm light for MP microscopy [12, 82, 92–95]. The longer excitation wavelength has several advantages for UV microscopy including less cytotoxicity and photobleaching, deeper specimen penetration and less light scattering. Apart from these advantages, the key benefit of using MP microscopy is its intrinsic sectioning capability since multiphoton events only occur in the focal plane [11, 96–99].

Schroeder, Webb, Gratton and colleagues, pioneered MP excitation microscopy of DHE [93]. Using an excitation wavelength of λ_{ex} = 920–930 nm, these authors visualized DHE in L-cell fibroblasts and found the sterol mainly in the plasma membrane and in lipid droplets (LDs) [93]. The published images were, however, of low quality (i.e., low signal-to-noise ratio, SNR), and no direct comparison to non-stained cells was made. The extremely low signal of DHE in MP microscopy is mostly a consequence of the low propensity of DHE for multiphoton excitation [11, 95]. Accordingly, high laser powers are required to obtain the necessary photon density at the focal point. We compared wide field and MP microscopy of DHE directly in the same samples and found that both methods provide similar information about sterol distribution [95]. Average laser powers in the range of 40–70 mW were required for MP excitation of DHE at λ_{ex} = 920 nm in CHO and HepG2 cells, and even then the images of DHE-stained cells were of low SNR. For comparison, two-photon excitation of enhanced green fluorescent protein at the same excitation wavelength required a laser power of only 0.3 mW [95]. One could also try to excite DHE more efficiently by a two-photon process using excitation wavelengths ≤700 nm. Our attempts to do that in cells, however, were unsuccessful due to overwhelming autofluorescence. Photobleaching of DHE is restricted to the focal plane in MP microscopy. Accordingly, we were able to acquire many frames (typically between 50 to 100) without significant intensity loss in MP microscopy of DHE. Although individual frames were of low SNR, averaging many frames increased the SNR dramatically. The frame-averaged MP image of DHE has a higher lateral resolution

than a corresponding single-frame image of the same specimen acquired on an epifluorescence microscope.

As has been reported for other fluorescent lipids, we did not find evidence for lateral domains of DHE in the plasma membrane of living cells by deconvolution of wide field microscopy images or by MP microscopy [53, 84, 95]. By both methods, fine cell protrusions in various cell types and sterol-containing nanotubes could be observed by microscopy of DHE. The need for frame averaging dramatically lowers the time-resolution of MP microscopy of DHE. While one image of DHE stained cells with good SNR can be acquired in less than 0.5 sec by widefield microscopy, a comparable image consists of about 30 averaged frames in MP microscopy, which requires between 1 to 2 min total acquisition time (depending on the pixel-dwell time) [95]. Accordingly, dynamic events occurring on a shorter time scale cannot be monitored and will result in motion-blurring. Despite the slow acquisition, this strategy has been used to record z-sections of DHE labeled CHO cells, and the sterol distribution in three dimensions could be observed [95].

In MP microscopy of DHE, a photomultiplier tube operating in photon-counting mode is used as the detector. In photon-counting the main source of noise in detection is the statistical uncertainty in the number of detected photons in a fixed time interval [100]. Computational progress in denoising routines allowed us to post-process individual frames of MP sequences of DHE stained cells achieving dramatic improvement in image quality [101,102]. After denoising MP microscopy images, we could follow the dynamics of individual vesicles containing DHE in living CHO cells with a time-resolution of 4 sec [101]. We found similar types of vesicle dynamics by wide field microscopy of DHE stained HepG2 and J774 cells [15, 53]. Since intracellular vesicles must contain significant amounts of DHE (about 3–5 mol%) to be detectable by either wide field or MP microscopy, both imaging modalities will only catch dynamics of sterol-enriched vesicles.

Analysis of intracellular sterol transport using fluorescence microscopy of Bodipy-cholesterol—As discussed earlier, BChol is the only fluorescent cholesterol analogue with an extrinsic fluorescence moiety that partitions preferentially into the I_o phase in model membranes [6, 7]. Thus, it fulfills an essential requirement of any suitable fluorescent analog of cholesterol. Co-labeling of M19 cells, a partial sterol-auxotroph Chinese hamster ovary (CHO) cell-line, with ^{3}H-cholesterol and BChol followed by sucrose density fractionation indicated a comparable distribution of cholesterol and BChol among cell membranes of varying equilibrium density [3]. Efflux of BChol from CHO cells to extracellular acceptors like BSA or apoA1 is significantly higher than that of cholesterol [3]. This is likely a consequence of the less efficient packing of phospholipid acyl chains around the BODIPY-moiety, as suggested by molecular dynamics simulations [3] and by studies in model membranes [4, 6, 7]. BChol becomes esterified by Raw264.7 macrophages after incubation with AcLDL, though with a lower efficiency than cholesterol [3]. By directly comparing transport of DHE and BChol, we found that both sterols are targeted to the endocytic recycling compartment (ERC), a major cellular sterol pool, with identical kinetics in baby hamster kidney (BHK) and in HeLa cells [7]. Uptake of DHE and BChol from the cell surface was strongly reduced in BHK cells overexpressing a dominant-negative clathrin heavy chain, and co-internalization of BChol with fluorescent transferrin, a marker for this uptake pathway, could be demonstrated [7]. These observations suggest that some plasma membrane sterol is internalized by clathrin-dependent endocytosis in these cells. By fluorescence lifetime imaging, we demonstrated that BChol's emission is constant throughout the cell, such that the fluorescence of this probe is a reliable measure of sterol concentration [7].

BChol has also been used to study sterol trafficking in CHO cells with defective Niemann-Pick C1 protein and to determine the role of oxysterol-binding protein-related proteins (ORPs) in cholesterol transport [3,103]. In the latter study, an impact of ORPs on transport of BChol from the plasma membrane to the ER and to LDs has been suggested using HeLa cells treated with oleic acid to stimulate droplet formation [103]. Importantly, we found that BChol is preferentially targeted to LDs in oleic-acid treated HeLa and BHK cells compared to DHE [7]. Low free cholesterol content of oleic-acid induced LDs in HeLa cells was recently confirmed by filipin staining by another group [104]. Thus, the preferred targeting of BChol to LDs compared to cholesterol or DHE indicates that the BODIPY-fluorophore affects the intracellular transport of BChol in cells with elevated fat content [7].

Based on our experience, we suggest using BChol exclusively for analysis of endocytic sterol trafficking, for example between plasma membrane and ERC. Moreover, we recommend performing co-localization studies of BChol with DHE by multi-color wide field microscopy, and only under conditions in which the probe distributions coincide, can one use the much better fluorescence properties of BChol for studies of sterol transport [7]. This is exemplified in Fig. 3, where cells were labeled with BChol using similar protocols as described for DHE in Box 2, and imaged on a multiphoton microscope. The intrinsic sectioning capability of this technique combined with negligible bleaching propensity outside the focal region enabled us to follow vesicles containing BChol over several hundred frames (Lund et al., manuscript in preparation). In this particular example, two dimly fluorescent vesicles form close to the brightly stained plasma membrane and fuse over a time course of a few minutes (Fig. 3B). If DHE would have been used instead of BChol, such vesicles would be hard to detect. Due to the much higher molecular brightness of BChol, we can detect it in intracellular membranes even after several rounds of vesicle fusion and fission (Lund et al., manuscript in preparation). In summary, BChol is useful as supplement to imaging of intrinsically fluorescent sterols in cells. In addition to its much better photo-physical properties, fluorescence imaging of BChol can be combined with electron microscopy studies making use of the diaminobenzidine reaction [105]. Upon illumination of BChol in glutaraldehyde or formaldehyde fixed cells, reactive oxygen species cause photo-oxidation of diaminobenzidine, thereby creating an electron-dense precipitate in sub-cellular regions where BChol is located [105, 106]. By this method, BChol was found in tubular endosomes, multivesicular bodies and the trans-Golgi network in human HepG2 hepatoma cells. The same approach has been used to follow the intracellular fate of BChol-oleate incorporated into high density lipoprotein [105]. A potential problem is the necessary fixation step, which, depending on the fixative and experimental conditions, can alter the intracellular sterol distribution.

Label-free imaging of sterols in model membranes and living cells

Ideally, one would like to visualize intracellular sterol distribution without the need for introducing labeled sterol probes. Two approaches for this that are being developed are reviewed here.

Sterol imaging by mass spectrometry—Imaging by mass spectrometry has been used to determine the steady state distribution of cholesterol and other membrane lipids based on chemically specific ionization patterns. Secondary ion mass spectrometry (SIMS) allows for detecting cholesterol and other biomolecules based on characteristic fragmentation patterns. Matrix-enhanced SIMS and time-of-flight SIMS were used to detect phospholipids and cholesterol in neuroblastoma cells and in tissue slices and to visualize cholesterol in cell attachment sites [107, 108]. Chemical mapping is typically limited by the low signal intensity from various biomolecules. Fragmentation of cholesterol in SIMS imaging typically provides several peaks in the mass range of the fragment ion m/z=366–370 which

can be used to visualize and quantify cellular cholesterol. Recently, a characteristic fragment of cholesterol of mass-charge ratio m/z= 147 has been used as a fingerprint to visualize cholesterol accumulation in J774 murine macrophages [109]. J774 cells pre-treated with MβCD-cholesterol [110] had about two times more cholesterol in the plasma membrane than control cells [109, 111]. For cellular cholesterol imaging by mass spectrometry, two major limitations need to be overcome; SIMS can be used only in freeze-dried samples, and the method has a spatial resolution approximating the cell diameter (i.e., at present no subcellular sterol distribution can be revealed). The technique might currently be useful for determining sterol distribution in model membranes and lipid monolayers, since domain sizes in these systems can be quite large [112–115].

Sterol imaging by vibrational microscopy—Raman scattering is due to inelastic scattering of light, which results in frequency shifts compared to the incident light. Scattered light of lower frequency ($\omega_S = \omega_p - \omega_R$) or increased frequency ($\omega_{AS} = \omega_p + \omega_R$) compared to the incident light are called Stokes and anti-Stokes components, respectively [116]. The frequencies ω_R are caused by molecular vibrations, which can be used to identify and characterize (bio)molecules. Since the Raman signal is very weak, application of this technique to bioimaging is severely limited. Nevertheless, the method combined with confocal detection has been used to characterize cholesterol esters in HeLa cells and macrophage foam cells [117]. Moreover, Raman spectroscopy has been used as diagnostic tool to detect breast cancer, and combined Raman and fluorescence microscopy were applied to characterize atherosclerotic plaques [118, 119].

A major technical improvement is coherent anti-Stokes Raman scattering (CARS). In CARS, two coherent light beams of frequency ω_1 and $\omega_2$are used to drive a Raman scattering of frequency ω_R, which results in scattering signals about 10^5 fold stronger than spontaneous Raman scattering [116, 120]. The coherent addition of anti-Stokes Raman scattering radiation from many molecular oscillators in the focal volume is responsible for the sensitivity of the technique. This paved the way for biomedical applications of CARS, and this technique has been used for analysis of neutral lipids (i.e., cholesteryl and triacylglycerol esters) in cytoplasmic lipid droplets of mammalian cells [121], *Drosophila melanogaster* [122] and *Caenorhabditis elegans* [123] with chemical specificity. Neutral lipids are particularly suitable for CARS analysis due to the abundance of C-H stretching vibrations [121]. Characteristic vibrations of saturated versus unsaturated fatty acyl chains allow monitoring of lipid remodeling during nutritional or genetic perturbations [123, 124]. Another advantage of CARS is its ease combination with non-linear fluorescence microscopy. For example in *C. elegans,* fat storage organelles have been visualized by CARS, while multiphoton fluorescence microscopy provided complementary information on autofluorescent gut granules in the same samples [123]. Quantitative CARS microscopy revealed heterogeneity in acyl chain saturation of LDs in individual adipocytes [125]. Despite the improvements in CARS, vibrational microscopy is limited to cellular regions with large stores of similar lipid species (e.g., lipid droplets), and CARS remains largely confined to detection of neutral lipids due the contribution of the C-H stretching and the C=C vibrations to the CARS signal. CARS microscopy has great potential to unravel the physico-chemical basis of membrane phase separation, with CARS combined with fluorescence microscopy to visualize cholesterol-mediated lipid demixing in supported membranes [126]. Finally, CARS microscopy has been combined with other non-linear optical imaging methods, like two-photon excitation and sum-frequency generation to monitor atherosclerotic lesions and plaque formation in aortas of ApoE-deficient mice [127, 128].

Concluding remarks

There has been considerable progress over the past decade in the ability to observe the distribution of sterols in cells and to measure their transport between organelles using optical microscopy methods. CTL and DHE are reasonably good analogs of cholesterol, and it seems unlikely that fluorescent analogs that are better cholesterol analogs will be developed. However, these molecules are not identical to cholesterol, and this caveat must always accompany studies using them in mammalian cells. (Of course, DHE is a natural yeast sterol, so it can be used with confidence in these cells and in sterol auxotrophs for which DHE and other ergosterols are suitable dietary sterols.) With improvements in instrumentation, particularly blue-sensitive EMCCD cameras, DHE and CTL can be imaged reasonably well even for time lapse studies. Multiphoton microscopy opens the possibility of determining the three dimensional distribution of these fluorescent sterols. The weak fluorescence brightness and rapid photobleaching of these fluorescent sterols has led to a long search for sterol derivatives with brighter, more photostable fluorescence. At present, Bchol seems to be the best choice among such sterol derivatives in terms of its distribution and transport in cells. Bchol is less like cholesterol than either DHE or CTL, so the investigator must make a choice among these sterols depending on available instrumentation and the goals of the experiment.

There is still a need for better methods to label endogenous cholesterol in cells or tissues. Both filipin and the cholesterol-binding toxins have been used for such purposes. As discussed in this chapter, within a limited range of conditions filipin can be validated as a linear indicator of cholesterol levels, but there are many instances in which filipin binds to other molecules or has a nonlinear response to cholesterol levels. The sterol binding toxins are generally nonlinear in their sterol response, but they may be useful for detecting high levels of cholesterol in membranes.

The label-free detection of cholesterol has promise for detecting endogenous cholesterol, but at present the methods available do not have sufficient resolution and/or sensitivity for studies of the subcellular distribution of cholesterol.

Acknowledgments

DW acknowledges funding by grants of the Lundbeck Foundation, the Danish Research Agency Forskningsstyrelsen, Forskningsrådet for Natur og Univers (FNU), and the Danish Research Agency Forskningsstyrelsen, Forskningsrådet for Sundhed og sygdom (FSS). FRM received support from NIH Grant R37-DK27083.

List of abbreviations

BHK	baby hamster kidney
BODIPY	Bora-diaza-indacene
Bchol	BODIPY-cholesterol
CHO	Chinese hamster ovary
CARS	coherent anti-Stokes Raman scattering
CTL	cholestatrienol
DHE	dehydroergosterol
EMCCD	electron multiplying charge couple device
ERC	endocytic recycling compartment

GUV	giant unilamellar vesicle
LD	lipid droplet
LSO	lysosomal storage organelle
MβCD	methyl-β-cyclodextrin
MP	multiphoton
NPC	Niemann-Pick disease type C
ORP	oxysterol-binding protein-related protein
PBS	phosphate buffered saline
SIMS	Secondary ion mass spectrometry

References

1. Mesmin B, Maxfield FR. Intracellular sterol dynamics. Biochim Biophys Acta. 2009; 1791:636–645. [PubMed: 19286471]
2. Wüstner, D. Intracellular cholesterol transport. In: Ehnholm, C., editor. Cellular lipid metabolism. Springer press; 2009. p. 157-190.
3. Hölttä-Vuori M, Uronen RL, Repakova J, Salonen E, Vattulainen I, Panula P, Li Z, Bittman R, Ikonen E. BODIPY-cholesterol: a new tool to visualize sterol trafficking in living cells and organisms. Traffic. 2008; 9:1839–1849. [PubMed: 18647169]
4. Shaw JE, Epand RF, Epand RM, Li Z, Bittman R, Yip CM. Correlated fluorescence-atomic force microscopy of membrane domains: structure of fluorescence probes determines lipid localization. Biophys J. 2006; 90:2170–2178. [PubMed: 16361347]
5. Chiantia S, Ries J, Chwastek G, Carrer D, Li Z, Bittman R, Schwille P. Role of ceramide in membrane protein organization investigated by combined AFM and FCS. Biochim Biophys, Acta. 2008; 1778:1356–1364. [PubMed: 18346453]
6. Ariola FS, Li Z, Cornejo C, Bittman R, Heikal AA. Membrane fluidity and lipid order in ternary giant unilamellar vesicles using a new bodipy-cholesterol derivative. Biophys J. 2009; 96:2696–2708. [PubMed: 19348752]
7. Wüstner D, Solanko LM, Sokol E, Lund FW, Garvik O, Li Z, Bittman R, Korte T, Herrmann A. Quantitative Assessment of Sterol Traffic in Living Cells by Dual Labeling with Dehydroergosterol and BODIPY-cholesterol. Chem Phys Lipids. 2011 In press.
8. Hao M, Lin SX, Karylowski OJ, Wüstner D, McGraw TE, Maxfield FR. Vesicular and non-vesicular sterol transport in living cells. The endocytic recycling compartment is a major sterol storage organelle. J Biol Chem. 2002; 277:609–617. [PubMed: 11682487]
9. Yeagle PL, Bensen J, Boni L, Hui SW. Molecular packing of cholesterol in phospholipid vesicles as probed by dehydroergosterol. Biochim Biophys Acta. 1982; 692:139–146.
10. Fischer RT, Stephenson FA, Shafiee A, FS. delta 5,7,9(11)-Cholestatrien-3 beta-ol: a fluorescent cholesterol analogue. Chem Phys Lipids. 1974; 36:1–14. [PubMed: 6518610]
11. Wüstner D. Following intracellular cholesterol transport by linear and non-linear optical microscopy of intrinsically fluorescent sterols. Curr Pharm Biotechnol. 2010 In press.
12. McIntosh AL, Atshaves BP, Huang H, Gallegos AM, Kier AB, Schroeder F. Fluorescence techniques using dehydroergosterol to study cholesterol trafficking. Lipids. 2008; 43:1185–1208. [PubMed: 18536950]
13. Mukherjee S, Zha X, Tabas I, Maxfield FR. Cholesterol distribution in living cells: fluorescence imaging using dehydroergosterol as a fluorescent cholesterol analog. Biophys J. 1998; 75:1915–1925. [PubMed: 9746532]
14. Wüstner D, Mondal M, Tabas I, Maxfield FR. Direct observation of rapid internalization and intracellular transport of sterol by macrophage foam cells. Traffic. 2005; 6:396–412. [PubMed: 15813750]

15. Wüstner D, Herrmann A, Hao M, Maxfield FR. Rapid nonvesicular transport of sterol between the plasma membrane domains of polarized hepatic cells. J Biol Chem. 2002; 277:30325–30336. [PubMed: 12050151]

16. Gimpl G. Cholesterol-protein interaction: methods and cholesterol reporter molecules. Subcell Biochem. 2010; 51:1–45. [PubMed: 20213539]

17. Qin C, Nagao T, Grosheva I, Maxfield FR, Pierini LM. Elevated plasma membrane cholesterol content alters macrophage signaling and function. Arterioscler Thromb Vasc Biol. 2006; 26:372–378. [PubMed: 16306428]

18. Orci L, Montesano R, Meda P, Malaisse-Lagae F, Brown D, Perrelet A, Vassalli P. Heterogeneous distribution of filipin--cholesterol complexes across the cisternae of the Golgi apparatus. Proc Natl Acad Sci U S A. 1981; 78:293–297. [PubMed: 7017713]

19. Steer CJ, Bisher M, Blumenthal R, Steven AC. Detection of membrane cholesterol by filipin in isolated rat liver coated vesicles is dependent upon removal of the clathrin coat. J Cell Biol. 1984; 99:315–319. [PubMed: 6145719]

20. Arthur JR, Heinecke KA, Seyfried TN. Filipin recognizes both GM1 and cholesterol in GM1 gangliosidosis mouse brain. J Lipid Res. 52:1345–1351. [PubMed: 21508255]

21. Sokolov A, Radhakrishnan A. Accessibility of cholesterol in endoplasmic reticulum membranes and activation of SREBP-2 switch abruptly at a common cholesterol threshold. J Biol Chem. 2010; 285:29480–29490. [PubMed: 20573965]

22. Peake KB, Vance JE. Defective cholesterol trafficking in Niemann-Pick C-deficient cells. FEBS Lett. 2010; 584:2731–2739. [PubMed: 20416299]

23. Pipalia NH, Huang A, Ralph H, Rujoi M, Maxfield FR. Automated microscopy screening for compounds that partially revert cholesterol accumulation in Niemann-Pick C cells. J Lipid Res. 2006; 47:284–301. [PubMed: 16288097]

24. Pipalia NH, Cosner CC, Huang A, Chatterjee A, Bourbon P, Farley N, Helquist P, Wiest O, Maxfield FR. Histone deacetylase inhibitor treatment dramatically reduces cholesterol accumulation in Niemann-Pick type C1 mutant human fibroblasts. Proc Natl Acad Sci USA. 2011; 108:5620–5625. [PubMed: 21436030]

25. Rosenbaum AI, Rujoi M, Huang AY, Du H, Grabowski GA, Maxfield FR. Chemical screen to reduce sterol accumulation in Niemann-Pick C disease cells identifies novel lysosomal acid lipase inhibitors. Biochim Biophys Acta. 2009; 1791:1155–1165. [PubMed: 19699313]

26. Rujoi M, Pipalia NH, Maxfield FR. Cholesterol pathways affected by small molecules that decrease sterol levels in Niemann-Pick type C mutant cells. PLoS One. 2010; 5:e12788. [PubMed: 20877719]

27. Rosenbaum AI, Maxfield FR. Niemann-Pick type C disease: molecular mechanisms and potential therapeutic approaches. J Neurochem. 2011; 116:789–795. [PubMed: 20807315]

28. Ohvo-Rekila H, Ramstedt B, Leppimaki P, Slotte JP. Cholesterol interactions with phospholipids in membranes. Prog Lipid Res. 2002; 41:66–97. [PubMed: 11694269]

29. Nagle JF, Tristram-Nagle S. Structure of lipid bilayers. Biochim et Biophys Acta. 2000; 1469:159–195.

30. Hofsass C, Lindahl E, Edholm O. Molecular dynamics simulations of phospholipid bilayers with cholesterol. Biophys J. 2003; 84:2192–2206. [PubMed: 12668428]

31. Lindahl E, Edholm O. Spatial and energetic-entropic decomposition of surface tension in lipid bilayers from molecular dynamics simulations. J Chem Phys. 2000; 113:3882–3893.

32. Henriksen J, Rowat AC, Brief E, Hsueh YW, Thewalt JL, Zuckermann MJ, Ipsen JH. Universal behavior of membranes with sterols. Biophys J. 2006; 90:1639–1649. [PubMed: 16326903]

33. Vist MR, Davis JH. Phase equilibria of cholesterol/dipalmitoylphosphatidylcholine mixtures: 2H nuclear magnetic resonance and differential scanning calorimetry. Biochemistry. 1990; 29:451–464. [PubMed: 2302384]

34. Ipsen JH, Karlstrom G, Mouritsen OG, Wennerstrom H, Zuckermann MJ. Phase equilibria in the phosphatidylcholine-cholesterol system. Biochim Biophys Acta. 1987; 905:162–172. [PubMed: 3676307]

35. Ahmed SN, Brown DA, London E. On the origin of sphingolipid/cholesterol-rich detergent-insoluble cell membranes: Physiological concentrations of cholesterol and sphingolipid induce

formation of a detergent-insoluble, liquid-ordered lipid phase in model membranes. Biochemistry. 1997; 36:10944–10953. [PubMed: 9283086]

36. Mukherjee S, Maxfield FR. Membrane domains. Annu Rev Cell Dev Biol. 2004; 20:839–866. [PubMed: 15473862]
37. Munro S. Lipid rafts: elusive or illusive? Cell. 2003; 115:377–388. [PubMed: 14622593]
38. Garvik O, Benediktsen P, Ipsen JH, Simonsen AC, Wüstner D. The fluorescent cholesterol analog dehydroergosterol induces liquid-ordered domains in model membranes. Chem Phys Lipids. 2008; 159:114–118. [PubMed: 19477318]
39. Solanko, LM.; Lund, FW.; Midtiby, HS.; Brewer, JR.; Li, Z.; Bittman, R.; Wüstner, D. Orientation of membrane-embedded BODIPY-cholesterol determined by two-photon polarization microscopy and Fourier-space image analysis. 2011. in preparation
40. Smutzer G, Crawford BF, Yeagle PL. Physical properties of the fluorescent sterol probe dehydroergosterol. Biochim et Biophys Acta. 1986; 862:361–371.
41. Rogers J, Lee AG, Wilton DC. The organisation of cholesterol and ergosterol in lipid bilayers based on studies using non-perturbing fluorescent sterol probes. Biochim Biophys Acta. 1979; 552:23–37. [PubMed: 435495]
42. Chong PL, Thompson TE. Depolarization of dehydroergosterol in phospholipid bilayers. Biochim Biophys Acta. 1986; 863:53–62. [PubMed: 3778912]
43. Yeagle PL, Albert AD, Boesze-Battaglia K, Young J, Frye J. Cholesterol dynamics in membranes. Biophys J. 1990; 57:413–424. [PubMed: 2306492]
44. Schroeder F, Nemecz G, Gratton E, Barenholz Y, Thompson TE. Fluorescence properties of cholestatrienol in phosphatidylcholine bilayer vesicles. Biophys Chem. 1988; 32:57–72. [PubMed: 3233314]
45. Hyslop PA, Morel B, Sauerheber RD. Organization and interaction of cholesterol and phosphatidylcholine in model bilayer membranes. Biochemistry. 1990; 29:1025–1038. [PubMed: 2160270]
46. Fischer RT, Stephenson FA, Shafiee A, Schroeder F. Structure and Dynamic Properties of Dehydroergosterol, delta 5,7,9(11),22-ergostatetraen-3 beta-ol. J Biol Chem. 1985; 13:13–24.
47. Schroeder F, Barenholz Y, Gratton E, Thompson TE. A fluorescence study of dehydroergosterol in phosphatidylcholine bilayer vesicles. Biochemistry. 1987; 26:2441–2448. [PubMed: 3607026]
48. Lakowitz, JR. Principles of fluorescence spectroscopy. Springer; New York, USA: 2006.
49. Wüstner D. Fluorescent sterols as tools in membrane biophysics and cell biology. Chem Phys Lipids. 2007; 146:1–25. [PubMed: 17241621]
50. Baumgart T, Hunt G, Farkas ER, Webb WW, Feigenson GW. Fluorescence probe partitioning between Lo/Ld phases in lipid membranes. Biochim Biophys Acta. 2007; 1768:2182–2194. [PubMed: 17588529]
51. Scheidt HA, Müller P, Herrmann A, Huster D. The potential of fluorescent and spin-labeled steroid analogs to mimic natural cholesterol. J Biol Chem. 2003; 278:45563–45569. [PubMed: 12947110]
52. Henriksen J, Rowat AC, Ipsen JH. Vesicle fluctuation analysis of the effects of sterols on membrane bending rigidity. Eur Biophys J. 2004; 33:732–741. [PubMed: 15221234]
53. Wüstner D, Færgeman NJ. Spatiotemporal analysis of endocytosis and membrane distribution of fluorescent sterols in living cells. Histochem Cell Biol. 2008; 130:891–908. [PubMed: 18787836]
54. Hartwig Petersen N, Færgeman NJ, Yu L, Wüstner D. Kinetic imaging of NPC1L1 and sterol trafficking between plasma membrane and recycling endosomes in hepatoma cells. J Lipid Res. 2008; 49:2023–2037. [PubMed: 18523240]
55. Mondal M, Mesmin B, Mukherjee S, Maxfield FR. Sterols are mainly in the cytoplasmic leaflet of the plasma membrane and the endocytic recycling compartment in CHO cells. Mol Biol Cell. 2009; 20:581–588. [PubMed: 19019985]
56. Kohut P, Wüstner D, Hronska L, Kuchler K, Hapala I, Valachovic M. The role of ABC proteins Aus1p and Pdr11p in the uptake of external sterols in yeast: Dehydroergosterol fluorescence study. Biochem Biophys Res Commun. 2011; 404:233–238. [PubMed: 21110944]
57. Li Z, Mintzer E, Bittman R. First synthesis of free cholesterol-BODIPY conjugates. J Org Chem. 2006; 71:1718–1721. [PubMed: 16468832]

58. Marks DL, Bittman R, Pagano RE. Use of Bodipy-labeled sphingolipid and cholesterol analogs to examine membrane microdomains in cells. Histochem Cell Biol. 2008; 130:819–832. [PubMed: 18820942]
59. Bergström F, Mikhalyov I, Hägglöf P, Wortmann R, Ny T, Johansson LB-Å. Dimers of Dipyrrometheneboron difluoride (BODIPY) with light spectroscopic applications in chemistry and biology. J Am Chem Soc. 2002; 124:196–204. [PubMed: 11782171]
60. Chen CS, Martin OC, Pagano RE. Changes in the spectral properties of a plasma membrane lipid analog during the first seconds of endocytosis in living cells. Biophys J. 1997; 72:37–50. [PubMed: 8994591]
61. Puri V, Watanabe R, Singh RD, Dominguez M, Brown JC, Wheatley CL, Marks DL, Pagano RE. Clathrin-dependent and -independent internalization of plasma membrane sphingolipids initiates two Golgi targeting pathways. J Cell Biol. 2001; 154:535–547. [PubMed: 11481344]
62. Pagano RE, Martin OC, Kang HC, Haugland RP. A novel fluorescent ceramide analogue for studying membrane traffic in animal cells: accumulation at the Golgi apparatus results in altered spectral properties of the sphingolipid precursor. J Cell Biol. 1991; 113:1267–1279. [PubMed: 2045412]
63. Puri V, Watanabe R, Dominguez M, Sun X, Wheatley CL, Marks DL, Pagano RE. Cholesterol modulates membrane traffic along the endocytic pathway in sphingolipid-storage diseases. Nat Cell Biol. 1999; 1:386–388. [PubMed: 10559968]
64. Sharma DK, Choudhury A, Singh RD, Wheatley CL, Marks DL, Pagano RE. Glycosphingolipids internalized via caveolar-related endocytosis rapidly merge with the clathrin pathway in early endosomes and form microdomains for recycling. J Biol Chem. 2003; 278:7564–7572. [PubMed: 12482757]
65. Sharma DK, Brown JC, Choudhury A, Peterson TE, Holicky E, Marks DL, Simari R, Parton RG, Pagano RE. Selective stimulation of caveolar endocytosis by glycosphingolipids and cholesterol. Mol Biol Cell. 2004; 15:3114–3122. [PubMed: 15107466]
66. Qin W, Baruah M, Van der Auweraer M, De Schryver FC, Boens N. Photophysical properties of borondipyrromethene analogues in solution. J Phys Chem A. 2005; 109:7371–7384. [PubMed: 16834104]
67. Aittoniemi J, Róg T, Niemelä P, Pasenkiewicz-Gierula M, Karttunen M, Vattulainen I. Tilt: major factor in sterols' ordering capability in membranes. J Phys Chem B. 2006; 110:25562–25564. [PubMed: 17181184]
68. Fischer RT, Cowlen MS, Dempsey ME, Schroeder F. Fluorescence of delta 5,7,9(11),22-ergostatetraen-3 beta-ol in micelles, sterol carrier protein complexes, and plasma membranes. Biochemistry. 1985; 24:3322–3331. [PubMed: 4027244]
69. Marsan MP, Muller I, Ramos C, Rodriguez F, Dufourc EJ, Czaplicki J, Milon A. Cholesterol orientation and dynamics in dimyristoylphosphatidylcholine bilayers: A solid state deuterium NMR analysis. Biophys J. 1999; 76:351–359. [PubMed: 9876147]
70. Craig IF, Via DP, Mantulin WW, Pownall HJ, Gotto AMJ, LCS. Low density lipoproteins reconstituted with steroids containing the nitrobenzoxadiazole fluorophore. J Lipid Res. 1981; 22:687–696. [PubMed: 7276743]
71. Reiner S, Micolod D, Schneiter R. Saccharomyces cerevisiae, a model to study sterol uptake and transport in eukaryotes. Biochem Soc Trans. 2005; 33:1186–1188. [PubMed: 16246078]
72. Loura LMS, Fedorov A, Prieto M. Exclusion of a cholesterol analog from the cholesterol-rich phase in model membranes. Biochim Biophys Acta. 2001; 1511:236–243. [PubMed: 11286966]
73. Wiegand V, Chang TY, Strauss JFr, Fahrenholz F, Gimpl G. Transport of plasma membrane-derived cholesterol and the function of Niemann-Pick C1 Protein. FASEB J. 2003; 17:782–784. [PubMed: 12594172]
74. Huang H, McIntosh AL, Atshaves BP, Ohno-Iwashita Y, Kier AB, Schroeder F. Use of dansyl-cholestanol as a probe of cholesterol behavior in membranes of living cells. J Lipid Res. 2010; 51:1157–1172. [PubMed: 20008119]
75. Shrivastava S, Haldar S, Gimpl G, Chattopadhyay A. Orientation and dynamics of a novel fluorescent cholesterol analogue in membranes of varying phase. J Phys Chem B. 2009; 113:4475–4481. [PubMed: 19249840]

76. Benson DM, Bryan J, Plant AL, Gotto AMJ, Smith LC. Digital imaging fluorescence microscopy: spatial heterogeneity of photobleaching rate constants in individual cells. J Cell Biol. 1985; 100:1309–1323. [PubMed: 3920227]
77. Fischer RT, Stephenson FA, Shafiee A, Schroeder F. delta 5,7,9(11)-Cholestatrien-3 beta-ol: a fluorescent cholesterol analogue. Chem Phys Lipids. 1984; 36:1–14. [PubMed: 6518610]
78. Fellmann P, Zachowski A, Devaux PF. Synthesis and use of spin-labeled lipids for studies of the transmembrane movement of phospholipids. Methods Mol Biol. 1994; 27:161–175. [PubMed: 8298689]
79. Breslow R, Zhang BL. Cholesterol recognition and binding by cyclodextrin dimers. Journal of the American Chemical Society. 1996; 118:8495–8496.
80. Krieger M. Reconstitution of the hydrophobic core of low-denstiy lipoprotein. Methods Enzymol. 1986; 128:608–613. [PubMed: 3724525]
81. Matyash V, Geier C, Henske A, Mukherjee S, Hirsh D, Thiele C, Grant B, Maxfield FR, Kurzchalia TV. Distribution and transport of cholesterol in Caenorhabditis elegans. Mol Biol Cell. 2001; 12:1725–1736. [PubMed: 11408580]
82. Wüstner D, Landt Larsen A, Færgeman NJ, Brewer JR, Sage D. Selective visualization of fluorescent sterols in Caenorhabditis elegans by bleach-rate based image segmentation. Traffic. 2010; 11:440–454. [PubMed: 20070610]
83. Georgiev AG, Sullivan DP, Kersting MC, Dittman JS, Beh CT, Menon AK. Osh Proteins Regulate Membrane Sterol Organization but Are Not Required for Sterol Movement Between the ER and PM. Traffic. 2011
84. Wüstner D. Plasma membrane sterol distribution resembles the surface topography of living cells. Mol Biol Cell. 2007; 18:211–228. [PubMed: 17065557]
85. Hale JE, Schroeder F. Asymmetric transbilayer distribution of sterol across plasma membranes determined by fluorescence quenching of dehydroergosterol. Eur J Biochem. 1982; 122:649–661. [PubMed: 7060596]
86. Wüstner D, Færgeman NJ. Chromatic aberration correction and deconvolution for UV sensitive imaging of fluorescent sterols in cytoplasmic lipid droplets. Cytometry A. 2008; 73:727–744. [PubMed: 18561197]
87. Swedlow JR. Quantitative fluorescence microscopy and image deconvolution. Methods in Cell Biology. 2007; 81:447–465. [PubMed: 17519179]
88. Young IT. Image fidelity: characterizing the imaging transfer function. Methods Cell Biol. 1989; 30:2–45.
89. Sibarita JB. Deconvolution microscopy. Adv Biochem Eng Biotechnol. 2005; 95:201–243. [PubMed: 16080270]
90. Markham J, Conchello JA. Artefacts in restored images due to intensity loss in three-dimensional fluorescence microscopy. J Microsc. 2001; 204:93–98. [PubMed: 11737542]
91. Wüstner D, Sage D. Multicolor bleach-rate imaging enlightens in vivo sterol transport. Commun Integr Biol. 2010; 3:1–4. [PubMed: 20539772]
92. McIntosh AL, Gallegos AM, Atshaves BP, Storey SM, Kannoju D, Schroeder F. Fluorescence and multiphoton imaging resolve unique structural forms of sterol in membranes of living cells. J Biol Chem. 2003; 278:6384–6403. [PubMed: 12456684]
93. Frolov A, Petrescu A, Atshaves BP, So PT, Gratton E, Serrero G, Schroeder F. High density lipoprotein-mediated cholesterol uptake and targeting to lipid droplets in intact L-cell fibroblasts. J Biol Chem. 2000; 275:12769–12780. [PubMed: 10777574]
94. Zhang W, McIntosh AL, Xu H, Wu D, Gruninger T, Atshaves B, Liu JC, Schroeder F. Structural analysis of sterol distributions in the plasma membrane of living cells. Biochemistry. 2005; 44:2864–2884. [PubMed: 15723530]
95. Wüstner D, Brewer JR, Bagatolli LA, Sage D. Potential of ultraviolet widefield imaging and multiphoton microscopy for analysis of dehydroergosterol in cellular membranes. Microsc Res Tech. 2011; 74:92–108. [PubMed: 21181715]
96. Zipfel WR, Williams RM, Webb WW. Nonlinear magic: multiphoton microscopy in the biosciences. Nat Biotechnol. 2003; 21:1369–1377. [PubMed: 14595365]

97. Masters, BR.; So, PTC. Classical and Quantum Theory of One-Photon and Multiphoton Fluorescence Spectroscopy. In: Masters, BR.; So, PTC., editors. Handbook of Biomedical Nonlinear Optical Microscopy. Oxford University Press; 2008. p. 91-152.

98. Xu, C.; Zipfel, WR. Multiphoton Excitation of Fluorescent Probes. In: Masters, BR.; So, PTC., editors. Handbook of Biomedical Nonlinear Optical Microscopy. Oxford University Press; 2008. p. 311-333.

99. Schrader M, Bahlmann K, Hell SW. Three-Photon-Excitation microscopy: theory, experiment and applications. Optik. 1997; 104:116–124.

100. Yazdanfar, S.; So, PT. Signal Detection and Processing in Nonlinear Optical Microscopes. In: Masters, BR.; So, PTC., editors. Handbook of Biomedical Nonlinear Optical Microscopy. Oxford University Press; 2008. p. 283-309.

101. Lund, FW.; Brewer, JR.; Lomholt, MA.; Luisier, F.; Sage, D.; Wüstner, D. Intracellular Sterol Tracking by Multiphoton Time-lapse Microscopy and PURE-LET image denoising. 2011. submitted for publication

102. Luisier, F. PhD thesis. EPFL; 2010. The SURE-LET Approach to Image Denoising. Thesis No. 4566

103. Jansen M, Ohsaki Y, Rita Rega L, Bittman R, Olkkonen VM, Ikonen E. Role of ORPs in sterol transport from plasma membrane to ER and lipid droplets in mammalian cells. Traffic. 2011; 12:218–231. [PubMed: 21062391]

104. Du X, Kumar J, Ferguson C, Schulz TA, Ong YS, Hong W, Prinz WA, Parton RG, Brown AJ, Yang H. A role for oxysterol-binding protein-related protein 5 in endosomal cholesterol trafficking. J Cell Biol. 2011; 192:121–135. [PubMed: 21220512]

105. Röhrl C, Meisslitzer-Ruppitsch C, Bittman R, Li Z, Pabst G, Prassl R, Strobl W, Neumüller J, Ellinger A, Pavelka M, Stangl H. Combined Light and Electron Microscopy using Diaminobenzidine Photooxidation to Monitor Trafficking of Lipids Derived from Lipoprotein Particles. Curr Pharm Biotechnol. 2011 In press.

106. Ellinger A, Vetterlein M, Weiss C, Meisslitzer-Ruppitsch C, Neumüller J, Pavelka M. High-pressure freezing combined with in vivo-DAB-cytochemistry: a novel approach for studies of endocytic compartments. J Struct Biol. 2010; 169:286–293. [PubMed: 19857575]

107. Altelaar AF, Klinkert I, Jalink K, de Lange RP, Adan RA, Heeren RM, Piersma SR. Gold-enhanced biomolecular surface imaging of cells and tissue by SIMS and MALDI mass spectrometry. Anal Chem. 2006; 78:734–742. [PubMed: 16448046]

108. Nygren H, Malmberg P. Silver deposition on freeze-dried cells allows subcellular localization of cholesterol with imaging TOF-SIMS. J Microsc. 2004; 215:156–161. [PubMed: 15315502]

109. Piehowski PD, Carado AJ, Kurczy ME, Ostrowski SG, Heien ML, Winograd N, Ewing AG. MS/MS methodology to improve subcellular mapping of cholesterol using TOF-SIMS. Anal Chem. 2008; 80:8662–8667. [PubMed: 18925746]

110. Zidovetzki R, Levitan I. Use of cyclodextrins to manipulate plasma membrane cholesterol content: evidence, misconceptions and control strategies. Biochim Biophys Acta. 2007:1768.

111. Ostrowski SG, Kurczy ME, Roddy TP, Winograd N, Ewing AG. Secondary ion MS imaging to relatively quantify cholesterol in the membranes of individual cells from differentially treated populations. Anal Chem. 2007; 79:3554–3560. [PubMed: 17428032]

112. Sostarecz AG, McQuaw CM, Ewing AG, Winograd N. Phosphatidylethanolamine-induced cholesterol domains chemically identified with mass spectrometric imaging. J Am Chem Soc. 2004; 126:13882–13883. [PubMed: 15506723]

113. Zheng L, McQuaw CM, Ewing AG, Winograd N. Sphingomyelin/phosphatidylcholine and cholesterol interactions studied by imaging mass spectrometry. J Am Chem Soc. 2007; 129:15730–15731. [PubMed: 18044889]

114. Boxer SG, Kraft ML, Weber PK. Advances in imaging secondary ion mass spectrometry for biological samples. Annu Rev Biophys. 2009; 38:53–74. [PubMed: 19086820]

115. Anderton CR, Lou K, Weber PK, Hutcheon ID, Kraft ML. Correlated AFM and NanoSIMS imaging to probe cholesterol-induced changes in phase behavior and non-ideal mixing in ternary lipid membranes. Biochim Biophys Acta. 2011; 1808:307–315. [PubMed: 20883665]

116. Potma, EO.; Xie, XS. Theory of Spontaneous and Coherent Raman Scattering. In: Masters, BR.; So, PTC., editors. Handbook of Biomedical Nonlinear Optical Microscopy. Oxford University Press; 2008. p. 164-190.

117. van Manen HJ, Otto C. Cholesterol esters are detected by Raman microspectroscopy in HeLa cells. J Raman Spectrosc. 2009; 40:117–118.

118. Haka AS, Volynskaya Z, Gardecki JA, Nazemi J, Shenk R, Wang N, Dasari RR, Fitzmaurice M, Feld MS. Diagnosing breast cancer using Raman spectroscopy: prospective analysis. J Biomed Optics. 2009; 14:054023.

119. Haka AS, Kramer JR, Dasari RR, Fitzmaurice M. Mechanism of ceroid formation in atherosclerotic plaque: in situ studies using a combination of Raman and fluorescence spectroscopy. J Biomed Optics. 2011; 16:011011.

120. Cheng JX, Jia YK, Zheng G, Xie XS. Laser-scanning coherent anti-Stokes Raman scattering microscopy and applications to cell biology. Biophys J. 2002; 83:502–509. [PubMed: 12080137]

121. Nan X, Cheng JX, Xie XS. Vibrational imaging of lipid droplets in live fibroblast cells with coherent anti-Stokes Raman scattering microscopy. J Lipid Res. 2003; 44:2202–2208. [PubMed: 12923234]

122. Chien CH, Chen WW, Wu JT, Chang TC. Label-free imaging of Drosophila in vivo by coherent anti-Stokes Raman scattering and two-photon excitation autofluorescence microscopy. J Biomed Optics. 2011; 16:016012.

123. Yen K, Le TT, Bansal A, Narasimhan SD, Cheng JX, Tissenbaum HA. A comparative study of fat storage quantitation in nematode Caenorhabditis elegans using label and label-free methods. PLoS One. 2010; 5:e12810. [PubMed: 20862331]

124. Mörck C, Olsen L, Kurth C, Persson A, Storm NJ, Svensson E, Jansson JO, Hellqvist M, Enejder A, Faergeman NJ, Pilon M. Statins inhibit protein lipidation and induce the unfolded protein response in the non-sterol producing nematode Caenorhabditis elegans. Proc Natl Acad Sci U S A. 2009; 106:18285–18290. [PubMed: 19826081]

125. Rinia HA, Burger KN, Bonn M, Müller M. Quantitative label-free imaging of lipid composition and packing of individual cellular lipid droplets using multiplex CARS microscopy. Biophys J. 2008; 95:4908–4914. [PubMed: 18689461]

126. Li L, Wang H, Cheng JX. Quantitative Coherent Anti-Stokes Raman Scattering Imaging of Lipid Distribution in Coexisting Domains. Biophys J. 2005; 89:3480–3490. [PubMed: 16126824]

127. Wang HW, Langohr IM, Sturek M, Cheng JX. Imaging and quantitative analysis of atherosclerotic lesions by CARS-based multimodal nonlinear optical microscopy. Arterioscler Thromb Vasc Biol. 2009; 29:1342–1348. [PubMed: 19520975]

128. Lim RS, Kratzer A, Barry NP, Miyazaki-Anzai S, Miyazaki M, Mantulin WW, Levi M, Potma EO, Tromberg BJ. Multimodal CARS microscopy determination of the impact of diet on macrophage infiltration and lipid accumulation on plaque formation in ApoE-deficient mice. J Lipid Res. 2010; 51:1729–1737. [PubMed: 20208058]

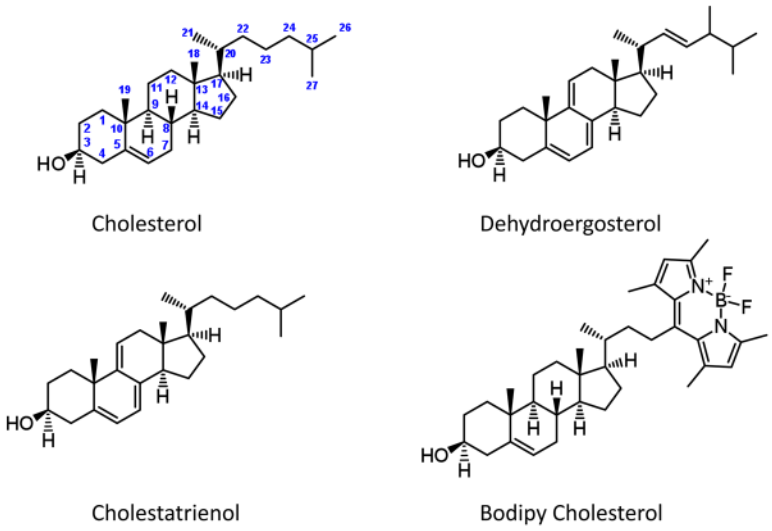

Figure 1.
Chemical structures of cholesterol, dehydroergosterol, cholestatrienol, and Bodipy-cholesterol.

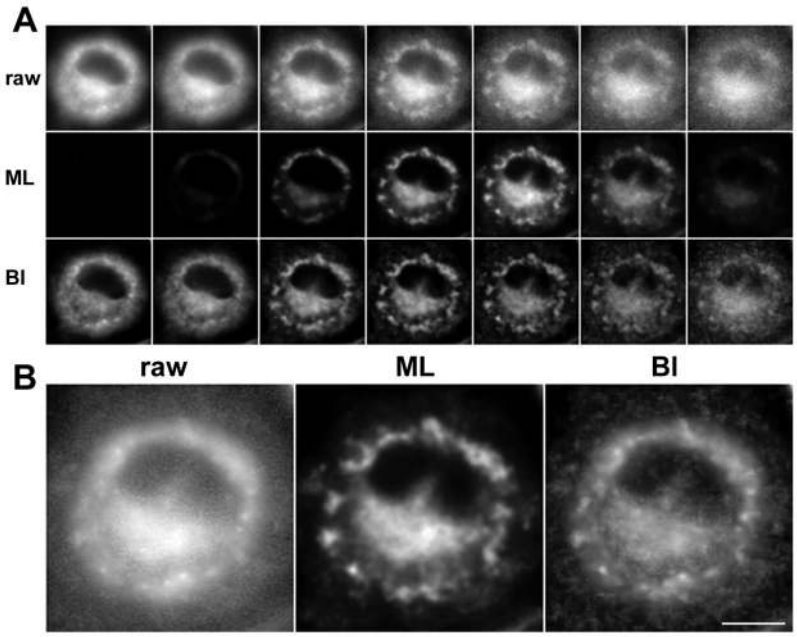

Figure 2. Image deconvolution improves analysis of DHE distribution in living cells

J774 macrophages were incubated with 10 μg/ml acetylated LDL for 6h to induce foam cell formation, washed and labeled for 5 min at 37°C with DHE/MβCD, as described in box 1 [14]. Cells were washed, chased for 30 min and imaged on a UV-sensitive wide field microscope. Ten images were acquired along the optical axis with 0.5 μm distance between the frames. The images were corrected for photobleaching along the stack, as described [86]. A, central 7 frames of the raw image stack, upper panel ('raw'), after applying maximum likelihood deconvolution implemented in Huygens software (Scientific Volume Imaging, Hilversum, The Netherlands) with a theoretical point spread function (PSF), middle panel ('ML'), the bleach-corrected image stack after applying a blind deconvolution as implemented in Autoquant (Media Cybernetics, Inc., Silver Spring, MD, USA), lower panel ('Bl'). The latter method estimates the PSF directly from the data. B, maximum intensity projection of the image stack shown in A for all three methods. Deconvolved images appear less blurred than the raw data set. Note that the ML deconvolution is most noise-suppressive and gives the best results for deconvolution of DHE image sets [86]. Bar, 5 μm.

Box 1

Labeling cells with filipin

1. Prepare a stock solution of filipin (25 mg/ml) in dimethylsulfoxide that has been treated with Molecular Sieves to remove water. This solution can be stored as aliquots at −20°C in tightly capped containers in a dessicated box. Thaw each aliquot in a dessicated container. Discard after use; do not refreeze.
2. Rinse cells with buffered saline, and fix with paraformaldehyde (1.5%).
3. Rinse again with buffered saline.
4. Incubate cells with filipin at a final concentration of 50 μg/ml in buffered saline for 45 minutes at room temperature.
5. Rinse cells three times with buffered saline.

6. Acquire images using 360/40 nm excitation and 480/40 nm emission filters with a 365 nm dichroic long pass filter. (Other similar UV filters should work.) It is very important to use a low level of excitation. Depending on lamp, filters, etc., you can attenuate excitation by 90% – 99% with a neutral density filter. This reduced excitation will slow photobleaching.

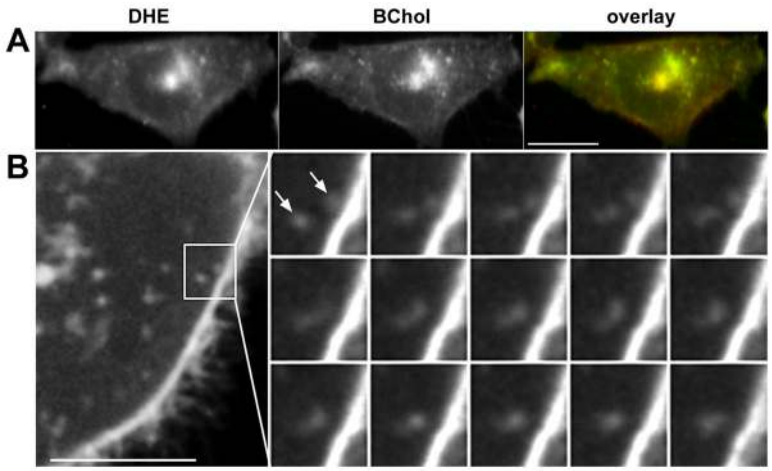

Figure 3. Multi-color sterol imaging and multiphoton time-lapse microscopy of BChol

A, CHO cells were pulse-labeled with DHE and BChol using a sterol/MβCD complex, washed and chased for 30 min at 37°C before imaging at a UV-sensitive wide field microscope, as described [7]. Left panel, DHE; middle panel, BChol; right panel, color overlay with DHE in red and BChol in green, respectively. B, HeLa cells were labeled with BChol/MβCD for 1 min at 37°C, washed and chased for 20 min at 37°C and placed on the nitrogen-floated stage of a home-built two-photon microscope. Images were acquired every 1 sec with an excitation wavelength of 930 nm for a total of 425 frames. Zoomed box in the large panel (left) shows two small BChol-containing vesicles (arrows), the upper just formed at the cell membrane (bright line on right half of the zoomed region). Over a time course of 15 sec, these two vesicles fuse (time montage on right panel). Bar, 10 μm in A, and 5 μm in B.